This document is the Accepted Manuscript version of a Published Work that appeared in final form in ACS Nano, copyright © American Chemical Society after peer review and technical editing by the publisher. To access the final edited and published work see: https://dx.doi.org/10.1021/acsnano.5b05071.

ACSNANO www.acsnano.org

ARTICLE

Synthesis of Nanoscale Coordination Polymers in Femtoliter Reactors on Surfaces

Mireia Guardingo,[†] Pablo González-Monje,[†] Fernando Novio,[†] Elena Bellido,[†,⊥] Félix Busqué,[‡] Gábor Molnár,[§] Azzedine Bousseksou,[§] and Daniel Ruiz-Molina*[,†]

[†]Catalan Institute of Nanoscience and Nanotechnology (ICN2), CSIC and The Barcelona Institute of Science and Technology, Campus UAB, Bellaterra 08193, Barcelona, Spain

[‡]Departament de Química, Universitat Autònoma de Barcelona (UAB), Campus UAB. Cerdanyola del Vallès 08193, Barcelona, Spain

[§]Laboratoire de Chimie de Coordination, Centre National de la Recherche Scientifique, 205, route de Narbonne, Toulouse 31077 Cedex 04, France

Supporting Information

ABSTRACT: **In the present work, AFM-assisted lithography was used to perform the synthesis of a coordination polymer inside femtoliter droplets deposited on surfaces. For this, solutions of the metal salt and the organic ligand were independently transferred to adjacent tips of the same AFM probe array and were sequentially delivered on the same position of the surface, creating femtoliter-sized reaction vessels where the coordination reaction and particle growth occurred. Alternatively, the two reagents were mixed in the cantilever array by loading an excess of the inks, and transferred to the surface immediately after, before the precipitation of the coordination polymer took place. The *in situ* synthesis allowed the reproducible obtaining of round-shaped coordination polymer nanostructures with control over their *XY* positioning on the surface, as characterized by microscopy and spectroscopy techniques.**

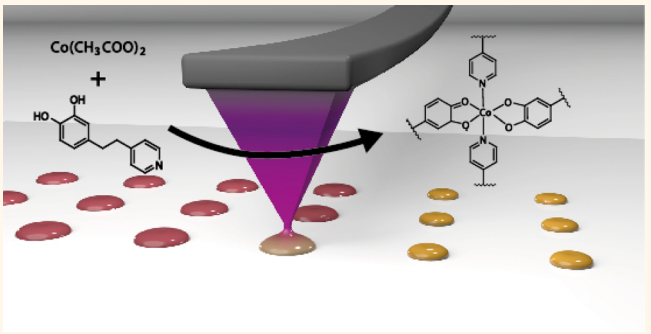

KEYWORDS: *nanoparticles, amorphous coordination polymers, synthesis on surfaces, femtoliter volumes, dip-pen nanolithography*

The controlled engineering of metal−organic nanostructures is a challenging area of growing interest. Beyond the design of molecular nanoarchitectures with well-defined and uniform sizes and morphologies, miniaturization is required in a number of novel and emerging application areas such as nanomedicine,[1,2] where nanoscale dimensions are necessary for the internalization of functional materials into cells,[3] or molecular electronics[4] where, if properly scaled down, each structure may represent a bit of information. Miniaturization can also improve colloidal dispersion, increase the surface area (and therefore the catalytic, sensing or storage capabilities), or fine-tune the physical properties of the materials.[5] One of the most common approaches for achieving a high degree of control over the dimensions of metal−organic materials consists in synthesizing them in nanoscale reactors.[6−11] Following this approach, synthesis in reverse microemulsions has become a widely extended practice[12] and a vast amount of Prussian-blue analogues and metal−organic frameworks (MOFs) with different shapes and sizes have been synthesized this way.[13−17] Self-enclosed structures have also been employed to obtain stimuli-responsive coordination nanomaterials. In fact, the first reported synthesis of spin-crossover nanoparticles made use of the water-in-oil technique,[18] and since then, multiple examples of particles with molecular switching properties have been described using synthesis in microdroplets.[19−22] Additionally, lab-on-a-chip approaches have also attracted much interest for fabricating coordination polymer nanostructures.[23]

Of special relevance is the synthesis of functional metal−organic nanostructures directly on surfaces,[24] due to the amount of potential applications that may arise upon their integration into functional hybrid devices. For this, the implementation of Dip-Pen Nanolithography (DPN, also known as direct-write atomic-force microscopy (AFM)-assisted lithography) arises as the most judicious choice as it allows to precisely position the materials or their precursors on specific areas of a surface.[25−27] Indeed, the piezoelectric-actuated positioning of the AFM can be used to achieve maximum control over the location of the functional materials, while the tip is used to deliver small volumes (femtoliters) of the precursor solutions (inks) to a specific target surface to form ultrasmall reactors.[28−32] So far DPN has allowed us to carry out

Received: August 14, 2015
Accepted: February 2, 2016

ACS Publications © XXXX American Chemical Society

DOI: 10.1021/acsnano.5b05071
ACS Nano XXXX, XXX, XXX−XXX

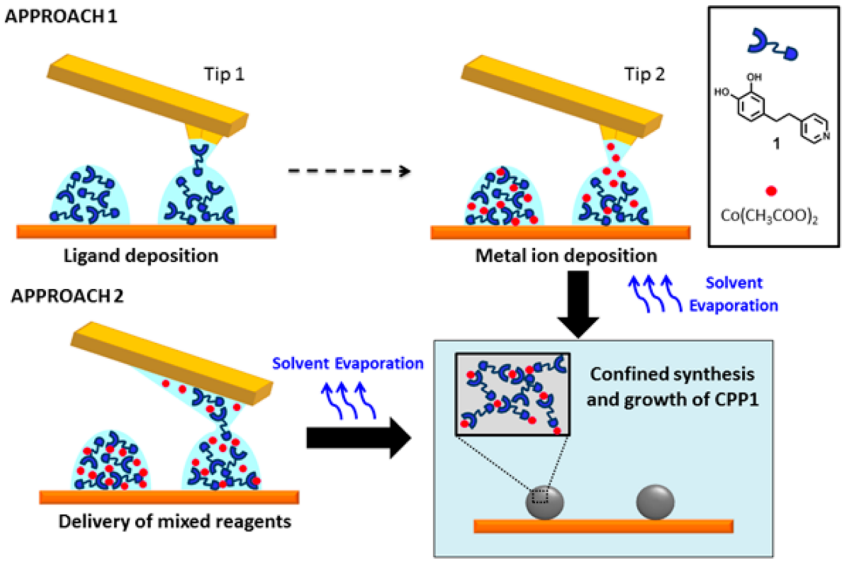

Figure 1. Schematic representation of the two experimental approaches followed in this work for the synthesis of a coordination polymer in femtoliter droplets assisted by an AFM tip. Approach 1: two different AFM tips were functionalized with the ligand (tip 1) and the metal salt (tip 2); the inks were mixed directly on the surface by sequentially delivering each one of the solutions to form femtoliter-sized reaction vessels. Approach 2: the two ink solutions were mixed in the cantilever array and the mixture was transferred to the surface where the reaction took place.

the direct deposition of magnetic coordination complexes on the most sensitive areas of superconducting sensors.[33−35] Our group also used DPN to control the growth of polyoxometalate nanostructures and crystals of the metal−organic framework HKUST-1 on precise positions of a surface.[36] Carbonell *et al.* also reported the crystal growth of the same HKUST-1 as well as the only example that, to our knowledge, has been reported so far regarding the synthesis of nanoscale MOFs directly on surface.[37,38] In these cases, the authors used a different tip-assisted lithographic technique known as Microfluidic Pen Lithography. Therefore, the *in situ* synthesis of coordination materials in femtoliter reactors on surfaces assisted by an AFM tip still represents a real scientific challenge.

Herein we describe how AFM tips functionalized with solutions containing a ditopic organic ligand and a metal salt can be used to induce a femtoliter-scale coordination polymerization reaction. As a proof-of-concept, we describe the successful site-directed synthesis of nanoscale coordination polymer particles (CPPs) on surfaces.[39] A schematic representation of the two approaches used in this work is shown in Figure 1. In Approach 1, two adjacent AFM tips of an array were differently coated with the organic ligand of choice (tip 1) and a metal salt solution (tip 2). Then, the coated tips were used to directly transfer the solutions to the surface in the shape of femtoliter droplets. Thanks to the precise positioning capability of the AFM, the two inks were mixed directly on the surface, creating femtoliter-sized reaction vessels where the coordination reaction occurred. In the second approach (Approach 2), an excess of ink was loaded on both tips during the coating procedure, forcing the reagents to mix on the cantilever array. The reacting mixture was immediately transferred to the surface before the precipitation of the CPPs occurred.

RESULTS AND DISCUSSION

The reaction of choice for these studies is based on a simplified protocol that employs only two reagents, *i.e.*, two inks. More specifically, it consists on the direct reaction of ligand **1**, which combines a catechol and a pyridine unit, with a cobalt salt (see Figure 1). As recently reported by our group,[40] this reaction yields nice round-shaped nanoscale particles (**CPP1**) when performed in solution using an EtOH/H_2O mixture, which however is not appropriate for DPN. In this technique, the ink solutions must fulfill several requirements: (i) the solutions must exhibit an adequate viscosity to ensure an homogeneous coating of the tip and a controlled transference of the material to the surface,[41] (ii) the inks must be in the liquid state throughout the whole writing process, (iii) the interplay of hydrophobic/hydrophilic interactions between the tip and the surface of interest mediated through the solvent of choice should be neither too weak nor too strong to guarantee a controlled delivery of the ink (according to our previous experience, optimal control over the lithographic process is achieved for contact angles (CA) of the ink solutions on the target surface of ∼80°; smaller CAs lead to a reduced control over the process as the spreading of the droplets on the surface is favored, whereas higher CAs make the delivery of the inks difficult), and (iv) the delivered materials should be highly soluble and stable in the solvents. Therefore, the first experimental steps were faced with having to reproduce the reaction in solution replacing the EtOH/H_2O mixture with solvents that satisfied the requirements of the lithographic technique.

Solvent Optimization. Initially, a parallel screening of the reaction using different solvents was carried out both in solution and by drop casting on surfaces using high boiling point solvents such as DMF, DMSO, H_2O and combinations of them. Small percentages of glycerol were added to the solutions in order to slow down the solvent evaporation rate while increasing the viscosity. Among all the different combinations assayed (see Supporting Information, S1 and S2 for details), the ink formulation that showed the best performance consisted of a mixture of $Co(CH_3COO)_2$ in Milli-Q water (100 mM, 1% glycerol) and ligand **1** in DMSO (200 mM, 2% glycerol).

DOI: 10.1021/acsnano.5b05071
ACS Nano XXXX, XXX, XXX−XXX

Mixing both solutions in bulk led to the immediate formation of a precipitate that was collected after stirring for 30 min, washed several times, and dried under vacuum. The characterization of the material by scanning electron microscopy (SEM) (see Figure 2a,b) revealed the formation of spherical particles with average mean diameter of 811 ± 27 nm. Simultaneously, drop casting experiments were performed using the same reagent solutions. For that, microliter volumes of each solution were successively deposited on gold surfaces using a micropipette and left to react at room temperature until the solvent evaporated. SEM images of the resulting structures revealed also the formation of round-shaped nanoparticles of approximately 214 ± 14 nm in diameter together with some nonstructured material (see Supporting Information, S3). It is worth mentioning here that all the attempts to directly deposit the nanoparticles synthesized in bulk through an AFM tip were unsuccessful. The SEM images of an AFM tip dipped in a **CPP1** suspension (see Supporting Information, S4) revealed the lack of nanoparticles on the probe and consequently on the deposited droplets. In fact, some of the larger objects that have been patterned using DPN are ferritin proteins with a size of *ca.* 12 nm.[42]

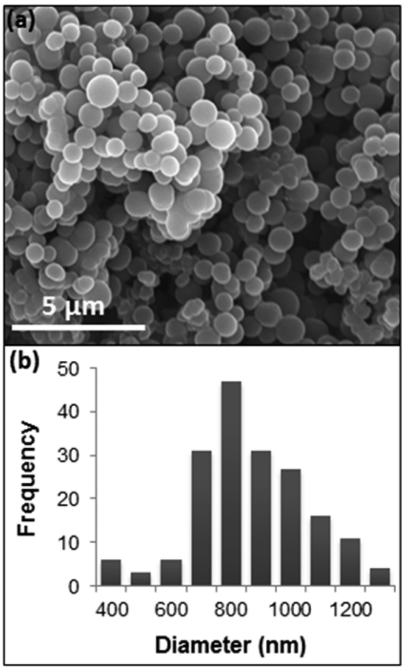

Figure 2. (a) SEM micrograph of CPP1 particles obtained in solution and the corresponding size distribution diagram (b).

Approach 1. The first experiments directed to synthesize **CPP1** particles in femtoliter droplets were carried out following the experimental methodology shown in Figure 3. In a typical experiment, a 200 mM solution of ligand **1** (4.3 mg) in DMSO (98 µL, 2 µL glycerol) and a 100 mM solution of $Co(CH_3COO)_2$ (3.5 mg) in H_2O (198 µL, 2 µL glycerol) were prepared and transferred to adjacent channels of a microfluidic ink delivery system (Inkwell, NanoInk). Commercial silicon nitride Type M Probe Arrays (66 µm pitch, also MP tips from NanoInk, Inc.) with a spring constant of 0.5 $N \cdot m^{-1}$ were afterward dipped in each solution, resulting in two tips functionalized differently with the ligand (tip 1) and the metal salt (tip 2) located side by side (Figure 3b). The coated tips were then brought into contact with a polycrystalline gold

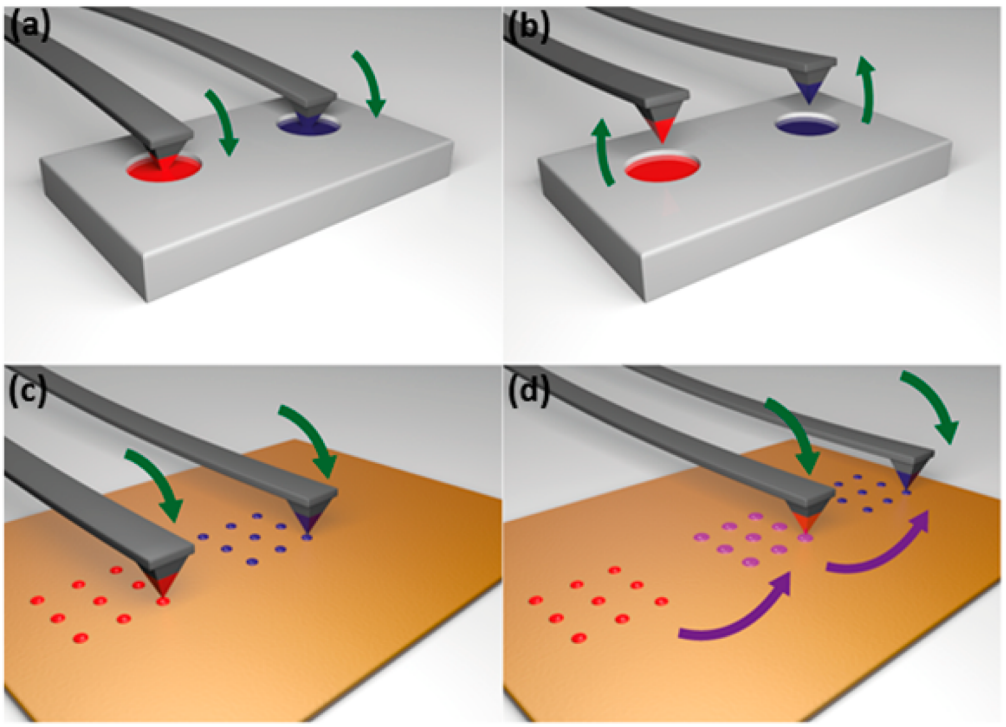

Figure Schematic representation of the reaction of $Co(CH_3COO)_2$ with ligand 1 through superimposed lithographies. (a and b) Two adjacent tips of a pen array were functionalized with ligand 1 (blue color, tip 1) and the metal salt (red color, tip 2). (c) Then, dot-like feature arrays were obtained over the gold surface with each one of the inks. (d) After a lateral movement of the tips, a second lithography was performed over the first one, which resulted in the mixture of the two inks and the fabrication of nanoscale reaction vessels (purple color) where the reaction and growth of the CPPs took place.

DOI: 10.1021/acsnano.5b05071
ACS Nano XXXX, XXX, XXX–XXX

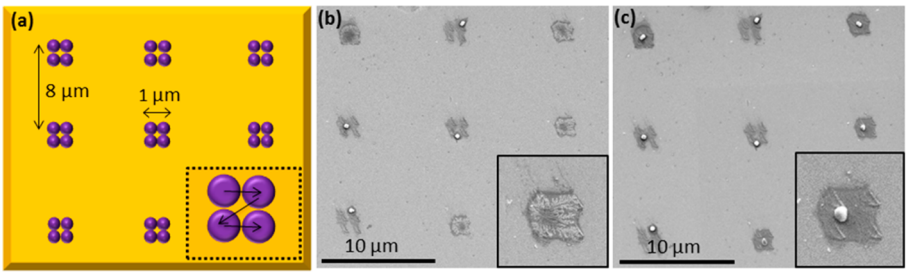

Figure 4. (a) Schematic representation of the 3 × 3 dot array used for the *in situ* synthesis and growth of CPP1 where each of the nine features was formed by four closely deposited droplets. After the writing process, each feature contained four droplets of the metal salt and four droplets of ligand 1. (b) SEM image of the different morphologies observed after exposing a substrate patterned as previously described to a DMSO atmosphere for 48 h (inset: detail of one of the dendritic-like structures formed at early stages). (c) SEM image of the particles grown in the same array stored under atmospheric conditions for 48 h after the first examination (inset: detail of the nanoparticle formed in the spot shown in the inset in panel b).

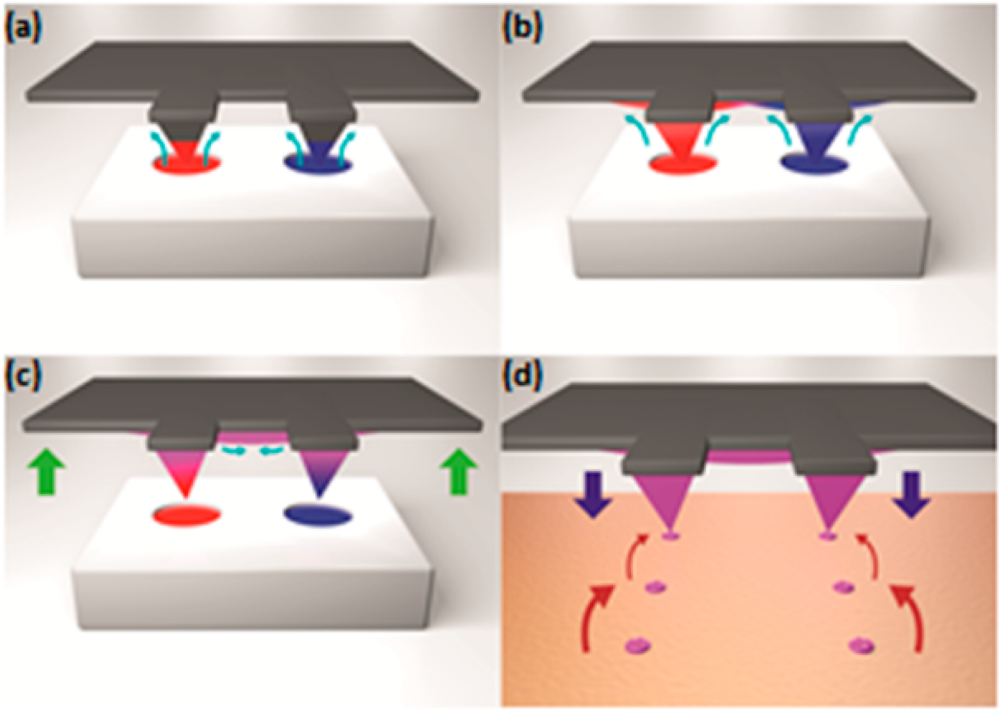

Figure 5. Schematic representation of the reaction of $Co(CH_3COO)_2$ with ligand 1 through the mixture of reagent solutions on the cantilever array (Approach 2). First, the tips were dipped in the inkwells (a) and were functionalized with each one of the inks (b). The use of an excessive loading of ink induced the mixture of the reagent solutions on the cantilever array (c), and then the reaction mixture was deposited on the surface during the early stages of the reaction, before the growth and precipitation of the CPPs took place (d).

surface to fabricate droplet arrays of the two separate solutions (Figure 3c). Finally, a lateral translation of the tips (66 μm) allowed to perform an additional lithography to deliver the second reagent over the first one (Figure 3d). In this way, femtoliter-sized droplets of the reacting mixture were fabricated *in situ* to act as nanoreactors. No significant effect of the reagent addition order was detected on the final morphology of the nanostructures; nevertheless, since the $Co(CH_3COO)_2$ ink demonstrated a higher writing stability, the mixtures were always performed by adding the metal over the ligand droplets. Importantly, the lithographies were carried out under high relative humidity conditions (~75%), and after the fabrication of the nanoreactors, the substrates were placed in an airtight chamber saturated with DMSO vapors for 48 h in order to avoid the rapid evaporation of the solvents, which usually resulted in the formation of unstructured material. However, this last step had to be carefully optimized since the exposure of the substrates to an overly saturated atmosphere led to the condensation of DMSO on the surface and the loss of the motifs (see Supporting Information, S5).

After performing several experiments, we observed that often the two ink solutions were positioned nearby but not exactly on top of each other, due to both the reduced dimensions of the ~~motives~~ and the implicit error of our experimental setup. In some cases, this led to the formation of nanoparticles only in the regions were the droplets overlapped (see Supporting Information, S6). To overcome this limitation, we designed a slightly modified lithographic pattern in which each reaction vessel was obtained by the fusion of four small droplets (a schematic representation of the new pattern is shown in Figure 4a). In this way, 3 × 3 dot arrays with each feature composed of four closely deposited droplets of each ink solution were fabricated. The substrates were then stored under a DMSO atmosphere for 2 days and examined by SEM. As shown in

DOI: 10.1021/acsnano.5b05071
ACS Nano XXXX, XXX, XXX−XXX

Figure 4b, after that time some of the mixed droplets showed the presence of rounded particles (with dimensions ranging from 375 to 485 nm in diameter) though others presented a dendritic-like material. That sample was then stored under atmospheric conditions for two additional days and examined again by SEM. Interestingly, after this time the dendritic-like features had evolved forming single particles with diameters ranging between 375 and 560 nm in each one of the mixed droplets (Figure 4c), with the appearance of some defects in specific experiments (see Supporting Information, S7).

For comparison purposes, the evolution of the reaction with time was also studied during the formation of **CPP1** in solution; to this end, a mixture of the reagent solutions was stirred for only 2 s and aliquots were collected at 5, 10, 30, and 120 s (SEM images of the resulting structures after solvent evaporation are shown in the Supporting Information, S8). Short reaction times led to the formation of wire-like structures formed by small granules growing in a dendritic-like conformation. Afterward, these progressively transformed into larger structures, initially lacking any defined morphology but finally resulting in the formation of round-shaped particles, in a process similar to that observed on surface. This fact may indicate that the formation mechanisms of the nanoparticles are similar in bulk and on surfaces.

Approach 2. The second approach designed for the synthesis of **CPP1** nanoparticles is schematically represented in Figure 5. First, the same ink solutions used in approach 1 were prepared and transferred to adjacent channels of a microfluidic ink delivery system. Afterward, Type M Probe Arrays were functionalized with them (Figure 5a). The inking procedure is always a critical step in DPN; by controlling parameters such as the tip pressure, dipping time, or position of the tips in the microchannels, we can control the ink loading. In this approach, we intentionally loaded large amounts of ink on the probes (Figure 5b) and forced the mixture of the two solutions on the cantilever array (Figure 5c). The coated tips were then used to directly transfer the mixture of inks onto the gold surface while maintaining the environmental relative humidity at ~75% (Figure 5d). In that way, the lithographic process was performed during the first stages of the reaction, just before the particles started to grow (see Supporting Information, S9).

It is worth to mention that, before the lithographic process could be performed, the ink excess had to be removed from the cantilevers by delivering large droplets of ink mixture onto the surface (bleeding step). The SEM images of the material formed in these large features revealed the formation of large amounts of spherical shaped particles with average diameters of 233 ± 15 nm (see Supporting Information, S10).

Once the ink excess was removed, the tips started writing uniform submicrometer sized droplet arrays. After the lithographic process, the substrates were placed in an airtight chamber saturated with DMSO vapors for 48 h in order to decrease the solvent evaporation rate. Alternatively, some samples were placed in an oven at 50 °C immediately after deposition, which led to similar results. Even though these two treatments may seem contradictory (a temperature increase is expected to induce faster evaporation rates), thermal treatment can also accelerate the reaction inside the vessels compensating for the fast evaporation of the solvents. As a representative example, Figure 6 shows the SEM image of one of such arrays composed of 25 features (5 × 5 dot array spaced by 8 μm) that was kept in a DMSO atmosphere after patterning. The image is

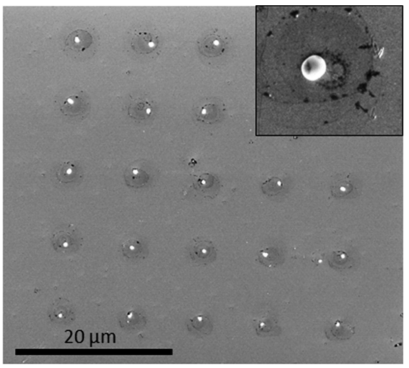

Figure 6. SEM image of the CPP1 particles obtained after the mixture of the inks on the cantilevers and grown on a droplet array (5 × 5) fabricated by traversing the tip over the surface. The growth of a single particle inside each deposited droplet was observed after keeping the patterned substrate under a DMSO saturated atmosphere for 48 h. The inset shows a magnified view of one of the obtained particles.

evidence of the growth of a single nanoparticle per dot with an average diameter of 445 ± 18 nm. Even though some imperfections appeared in specific experiments (see Supporting Information S11), the formation of one particle per dot showed good reproducibility (see Supporting Information, S12).

Finally, we observed that the volume of the deposited droplets directly influenced the final size of the CPPs. In Figure 7 we show three arrays fabricated in series where the volume of the deposited droplets decreased with the successive lithographies due to depletion of the ink (optical microscopy image, top row). Accordingly, the average size of the particles formed in the arrays after placing the sample in the oven at 50 °C systematically decreased with the successive lithographies, as shown in Figure 7. Particle diameters range from 450 to 630 nm for the array deposited first, whereas diameters from 280 to 390 nm and 230 to 330 nm were found for the second and third lithographies, respectively (see also Supporting Information, S13 for high resolution images of the complete arrays). This observation is consistent with results previously reported for the synthesis of coordination polymers into reverse micelles, which showed high monodispersion in size.[19,20]

Spectroscopic characterization. The nanoparticles synthesized on surface were characterized using Grazing Angle Infrared Spectroscopy (GA-IR) and MicroRaman Spectroscopy. First, the GA-IR spectra of drop-casted samples were compared to those of the bulk material showing good agreement (Figure 8a). In both cases, we observed the presence of a C−O stretching band from the catechol groups (~1230 cm^{-1}, doublet), a pyridine band centered at 1485 cm^{-1} ($\upsilon_{C=C/C-N}$), and the skeletal vibrations of the aromatic rings appearing at approximately 1600 cm^{-1}. Further comparison with the spectrum of the pure ligand **1** revealed an additional shift of the bands, attributed to the coordination to cobalt (ν_{C-O} doublet separation and increased intensity of the $\nu_{C=C/C-N}$; see Supporting Information, S14). We also succeeded in characterizing the material deposited in the large droplets generated during the bleeding of the cantilevers (after functionalization by approach 2) (Figure 8a). The GA-IR spectrum showed the same characteristic peaks as those previously found for the bulk **CPP1** nanoparticles, confirming the formation of the desired material on surface.

DOI: 10.1021/acsnano.5b05071
ACS Nano XXXX, XXX, XXX−XXX

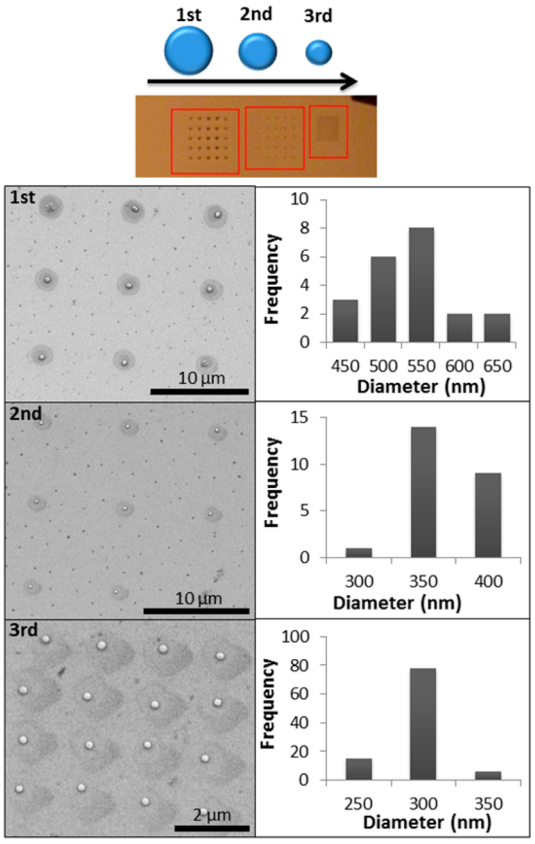

Figure 7. Optical microscopy image (top) showing a decrease of the deposited volume in arrays fabricated successively. Left column: SEM images of the particles obtained inside each one of the arrays after the substrate was placed in an oven at 50 °C. Right column: the particle diameter measurements denote a reduction in size associated with the decrease in deposited volume.

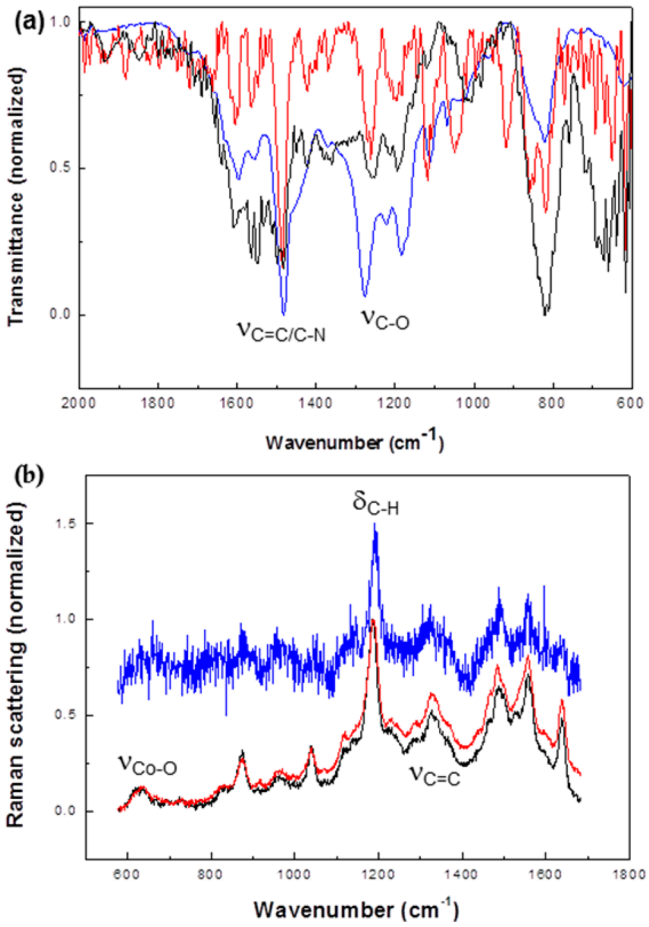

Figure 8. (a) GA-IR spectra of the CPPs obtained in solution (blue), in a drop-casting experiment (red), and in large drops obtained during the bleeding of the cantilevers using approach 2 (black). (b) Raman spectra of the CPPs synthesized in bulk (black), those obtained inside the cantilever bleeding droplets after following approach 2 (red), and [illegible] ones grown in individual reactors in patterned areas (blue). It can be observed that the spectrum obtained in the patterned area has a poor signal-to-noise ratio, but the high intensity bands can be distinguished.

Finally, MicroRaman spectroscopy was used as an additional characterization technique. The spectra were recorded in the 1700−500 cm^{-1} range in bulk samples as well as in droplets generated by DPN. The spectra obtained in the large drops deposited by approach 2 were in good agreement with the spectrum of the material obtained in bulk (Figure 8b). We could distinguish the bands associated with aromatic moieties (1480, 1190 cm^{-1}) and also the band corresponding to the stretching of the Co−O bond (640 cm^{-1}), which confirms the coordination of the metal to the catechol ring. The extremely small amount of material present in the patterned areas fabricated by approaches 1 and 2 (one particle grown inside each droplet) complicated the task of characterizing the CPPs grown in individual nanoreactors due to the large noise-to-signal ratio of the spectrum. However, after subtraction of the baseline, the most intense bands were clearly observed in the spectrum recorded over an area with a high density of particles (100 single particles in a 20 × 20 μm^2 area), as shown in Figure 8b. These bands were coincident with the bulk material, suggesting the formation of **CPP1** particles.

CONCLUSIONS

In this article, we have reported the *in situ* synthesis of coordination polymer particles inside femtoliter reactors deposited on surfaces using DPN. This was performed either by direct mixing of femtoliter droplets of the reagents through sequential delivery of the reagents or by premixing them on the cantilever array. Beyond achieving precise control over the *XY* positioning of the CPPs, the experimental methodology employed allowed us to promote in a reproducible manner the growth of a single nanostructure in each droplet with good monodispersion and tunable dimensions, which in our view represents a real breakthrough at the interface of nanotechnology and chemistry. Morphological and chemical characterization confirmed the reproducibility of the reaction at the femtoliter scale. Although there is still much research to be developed before this and other similar methodologies can be applied to the fabrication of functional devices, our work demonstrates the feasibility of our approach for the synthesis of coordination materials on surfaces and their integration into functional hybrid devices.

EXPERIMENTAL SECTION

Materials. Cobalt(II) acetate tetrahydrate (≥98%) and glycerol (≥99%) were purchased from Sigma-Aldrich, whereas ethanol absolute (EtOH, Sps, >99.8%), dimethyl sulfoxide (DMSO, Sps, >99.9%), and dimethylformamide (DMF, Sps, >99.9%) were purchased from Romil and acetone (HPLC, >99.9%) from Fischer. All the materials were

DOI: 10.1021/acsnano.5b05071
ACS Nano XXXX, XXX, XXX−XXX

used as received. Mili-Q water (18.2 mΩ·cm) was used in all cases. Ligand **1** was synthesized as described elsewhere.[39]

Synthesis of CPP1 in Bulk. An aqueous solution (1 mL) of $Co(CH_3COO)_2{\cdot}4H_2O$ (60.7 mg, 0.25 mmol) was added dropwise to a solution of ligand **1** (108.0 mg, 0.5 mmol) in DMSO (5 mL) under continuous gentle magnetic stirring, and immediately, a black precipitate was formed. After 30 min, the precipitate was centrifuged, washed several times with water and EtOH, and dried under vacuum. The resulting solid product was obtained in 65% yield.

Substrate Preparation. Silicon bearing a native oxide layer (Si/SiO_2) of substrates (0.5 × 0.5 cm) was washed in an ultrasonic bath for 10 min in acetone, absolute ethanol, and Milli-Q water and dried by blowing nitrogen. The clean Si/SiO_2 chips were then used to prepare gold substrates by Physical Vapor Deposition (PVD) of a 10 nm-thick adhesion layer (Ti or Cr, 99.99%) and a 40 nm layer of Au (99.99%). An Electron Beam Evaporator (from AJA International, Inc.) operating at an evaporation rate of 1 $Å{\cdot}s^{-1}$ and a base pressure of $\sim 10^{-7}$ Torr was used.

Drop-Casting Experiments. As a first step of the reaction miniaturization, several drop-casting experiments were performed. In general, the experiments consisted in sequentially adding microliter volumes of metal and ligand solutions onto a gold substrate and allowing the solvents to evaporate. Aqueous $Co(CH_3COO)_2{\cdot}4H_2O$ solutions (34 mM) and either DMSO or DMF solutions of ligand **1** (20 mM) containing 0−2% of glycerol were used, and the volume of each droplet was calculated in order to mix the two reagents in stoichiometric ratios (2:1 ligand/metal ratio). In all cases, the formation of spherical CPPs was observed after examination by FE-SEM.

AFM-Assisted Lithography Experiments. These experiments were performed using an Nscriptor DPN System (from NanoInk, Inc.). During all the droplet deposition processes, the relative humidity was kept constant at ∼75% using an environmental chamber integrated in the Nscriptor DPN System. Tips specially designed for writing purposes were used in all the lithographies, specifically, commercial silicon nitride Type M Probe Arrays (also MP tips from NanoInk, Inc.) with a spring constant of 0.5 $N{\cdot}m^{-1}$ and a tip radius of ∼15 nm. To coat the tips, a microfluidic ink delivery chip-based system (Inkwell, from NanoInk, Inc.) was used. In our experiments, contiguous channels of the inkwells were filled with the two ink solutions, and the tips were functionalized with them in a way that they either functionalized each tip separately (approach 1) or they mixed in the cantilever during the process (approach 2). After the deposition of the droplets, the substrates were kept in closed vessels saturated with DMSO vapors (a droplet of DMSO was positioned on a piece of filter paper and introduced in the chamber) or placed in an oven at 50 °C in order to control the solvent evaporation rate and the reaction velocity.

Characterization Methods. SEM images were obtained in a Quanta 650 FEG from FEI operating at 5 kV or a Magellan 400L also from FEI operating at 2 kV. The particles were measured using ImageJ and the diameter data are given from the Feret diameter. Grazing Angle Reflection IR Spectroscopy (GA-IR) analysis was performed using an Hyperion 2000 FT-IR microscope coupled to a Vertex 80 spectrophotometer. The instrument is equipped with an MCT nitrogen-cooled detector with the angle of incidence fixed at 83°. The ATR-IR spectra were recorded in a Tensor 27 (Bruker) combined with an ATR MKII Golden Gate accessory.

MicroRaman Spectroscopy. Raman spectra were acquired at room temperature using a Dilor triplemate spectrograph (1800 1 mm grating, 100 Lm entrance slit, 1 cm^{-1} spectral resolution) coupled to a Princeton Instruments CCD detector. The 647.1 nm line of a Kr^+ laser (Coherent Radiation Innova) was used as an excitation source with laser power output of 10 mW. The laser beam was focused on a spot approximately 3 mm in diameter and the Raman signal was collected in a backscattering geometry.

ASSOCIATED CONTENT

Supporting Information

The Supporting Information is available free of charge on the ACS Publications website at DOI: 10.1021/acsnano.5b05071.

Additional SEM images of solution samples, drop-cast samples and patterns and additional spectra (PDF)

AUTHOR INFORMATION

Corresponding Author

*E-mail: druiz@cin2.es.

Present Address

⊥Nanobiosciences Unit, Joint Research Centre, Institute for Health and Consumer Protection, European Commission, T.P.500, Via Enrico Fermi 2749, 21027 Ispra, VA, Italy.

Notes

The authors declare no competing financial interest.

ACKNOWLEDGMENTS

F. Novio thanks the Spanish Ministry (MINECO) for a Juan de la Cierva postdoctoral grant. M. Guardingo thanks CSIC for a predoctoral grant. This work was supported by project MAT2012-38318-C03-02, CTQ2010.-15380/BQU and CTQ2013.-41161-R from the Spanish Government and FEDER funds. Authors also thank MP1202 Cost Action. ICN2 acknowledges support from the Severo Ochoa Program (MINECO, Grant SEV-2013-0295).

REFERENCES

(1) Novio, F.; Simmchen, J.; Vázquez-Mera, N.; Amorín-Ferré, L.; Ruiz-Molina, D. Coordination Polymer Nanoparticles in Medicine. *Coord. Chem. Rev.* **2013**, *257*, 2839−2847.

(2) Horcajada, P.; Chalati, T.; Serre, C.; Gillet, B.; Sebrie, C.; Baati, T.; Eubank, J. F.; Heurtaux, D.; Clayette, P.; Kreuz, C.; Chang, J.-S.; Hwang, Y. K.; Marsaud, V.; Bories, P.-N.; Cynober, L.; Gil, S.; Férey, G.; Couvreur, P.; Gref, R. Porous Metal-Organic-Framework Nanoscale Carriers as a Potential Platform for Drug Delivery and Imaging. *Nat. Mater.* **2010**, *9*, 172−178.

(3) Novio, F.; Lorenzo, J.; Nador, F.; Wnuk, K.; Ruiz-Molina, D. Carboxyl Group (CO_2H) Functionalized Coordination Polymer Nanoparticles as Efficient Platforms for Drug Delivery. *Chem. - Eur. J.* **2014**, *20*, 15443−15450.

(4) Imaz, I.; Maspoch, D.; Rodríguez-Blanco, C.; Pérez-Falcón, J.; Campo, J.; Ruiz-Molina, D. Valence-Tautomeric Metal-Organic Nanoparticles. *Angew. Chem., Int. Ed.* **2008**, *47*, 1857−1860.

(5) Bousseksou, A.; Molnár, G.; Salmon, L.; Nicolazzi, W. Molecular Spin Crossover Phenomenon: Recent Achievements and Prospects. *Chem. Soc. Rev.* **2011**, *40*, 3313−3335.

(6) Falcaro, P.; Ricco, R.; Doherty, C. M.; Liang, K.; Hill, A. J.; Styles, M. J. MOF Positioning Technology and Device Fabrication. *Chem. Soc. Rev.* **2014**, *43*, 5513−5560.

(7) Doherty, C. M.; Buso, D.; Hill, A. J.; Furukawa, S.; Kitagawa, S.; Falcaro, P. Using Functional Nano- and Microparticles for the Preparation of Metal-Organic Framework Composites with Novel Properties. *Acc. Chem. Res.* **2014**, *47*, 396−405.

(8) Gentili, D.; Cavallini, M. Wet-Lithographic Processing of Coordination Compounds. *Coord. Chem. Rev.* **2013**, *257*, 2456−2467.

(9) Zhuang, J. L.; Ar, D.; Yu, X. J.; Liu, J. X.; Terfort, A. Patterned Deposition of Metal-Organic Frameworks onto Plastic, Paper, and Textile Substrates by Inkjet Printing of a Precursor Solution. *Adv. Mater.* **2013**, *25*, 4631−4635.

(10) Valtchev, V.; Tosheva, L. Porous Nanosized Particles: Preparation, Properties, and Applications. *Chem. Rev.* **2013**, *113*, 6734−6760.

DOI: 10.1021/acsnano.5b05071
ACS Nano XXXX, XXX, XXX−XXX

(11) Falcaro, P.; Buso, D.; Hill, A. J.; Doherty, C. M. Patterning Techniques for Metal Organic Frameworks. *Adv. Mater.* **2012**, *24*, 3153−3168.
(12) Ganguli, A. K.; Ganguly, A.; Vaidya, S. Microemulsion-Based Synthesis of Nanocrystalline Materials. *Chem. Soc. Rev.* **2010**, *39*, 474−485.
(13) Vaucher, S.; Li, M.; Mann, S. Synthesis of Prussian Blue Nanoparticles and Nanocrystal Superlattices in Reverse Microemulsions. *Angew. Chem., Int. Ed.* **2000**, *39*, 1793−1796.
(14) Dumont, M. F.; Risset, O. N.; Knowles, E. S.; Yamamoto, T.; Pajerowski, D. M.; Meisel, M. W.; Talham, D. R. Synthesis and Size Control of Iron(II) Hexacyanochromate(III) Nanoparticles and the Effect of Particle Size on Linkage Isomerism. *Inorg. Chem.* **2013**, *52*, 4494−4501.
(15) Roy, X.; Hui, J. K. H.; Rabnawaz, M.; Liu, G.; MacLachlan, M. J. Prussian Blue Nanocontainers: Selectively Permeable Hollow Metal-Organic Capsules from Block Ionomer Emulsion-Induced Assembly. *J. Am. Chem. Soc.* **2011**, *133*, 8420−8423.
(16) Liang, G.; Xu, J.; Wang, X. Synthesis and Characterization of Organometallic Coordination Polymer Nanoshells of Prussian Blue Using Miniemulsion Periphery Polymerization (MEPP). *J. Am. Chem. Soc.* **2009**, *131*, 5378−5379.
(17) Rieter, W. J.; Taylor, K. M. L.; An, H.; Lin, W.; Lin, W. Nanoscale Metal-Organic Frameworks as Potential Multimodal Contrast Enhancing Agents. *J. Am. Chem. Soc.* **2006**, *128*, 9024−9025.
(18) Forestier, T.; Mornet, S.; Daro, N.; Nishihara, T.; Mouri, S.; Tanaka, K.; Fouché, O.; Freysz, E.; Létard, J.-F. Nanoparticles of Iron(II) Spin-Crossover. *Chem. Commun.* **2008**, 4327−4329.
(19) Volatron, F.; Catala, L.; Rivière, E.; Gloter, A.; Stéphan, O.; Mallah, T. Spin-Crossover Coordination Nanoparticles. *Inorg. Chem.* **2008**, *47*, 6584−6586.
(20) Boldog, I.; Gaspar, A. B.; Martínez, V.; Pardo-Ibañez, P.; Ksenofontov, V.; Bhattacharjee, A.; Gütlich, P.; Real, J. A. Spin-Crossover Nanocrystals with Magnetic, Optical, and Structural Bistability Near Room Temperature. *Angew. Chem., Int. Ed.* **2008**, *47*, 6433−6437.
(21) Coronado, E.; Galán-Mascarós, J. R.; Monrabal-Capilla, M.; García-Martínez, J.; Pardo-Ibáñez, P. Bistable Spin-Crossover Nanoparticles Showing Magnetic Thermal Hysteresis near Room Temperature. *Adv. Mater.* **2007**, *19*, 1359−1361.
(22) Galán-Mascarós, J. R.; Coronado, E.; Forment-Aliaga, A.; Monrabal-Capilla, M.; Pinilla-Cienfuegos, E.; Ceolin, M. Tuning Size and Thermal Hysteresis in Bistable Spin Crossover Nanoparticles. *Inorg. Chem.* **2010**, *49*, 5706−5714.
(23) Puigmartí-Luis, J. Microfluidic Platforms: A Mainstream Technology for the Preparation of Crystals. *Chem. Soc. Rev.* **2014**, *43*, 2253−2271.
(24) Molnár, G.; Cobo, S.; Real, J. A.; Carcenac, F.; Daran, E.; Vieu, C.; Bousseksou, A. A Combined Top-Down/bottom-up Approach for the Nanoscale Patterning of Spin-Crossover Coordination Polymers. *Adv. Mater.* **2007**, *19*, 2163−2167.
(25) Perevedentsev, A.; Sonnefraud, Y.; Belton, C. R.; Sharma, S.; Cass, A. E. G.; Maier, S. A.; Kim, J.; Stavrinou, P. N.; Bradley, D. D. C. Dip-Pen Patterning of Poly(9,9-dioctylfluorene) Chain-Conformation-Based Nano-Photonic Elements. *Nat. Commun.* **2015**, *6*, 5977.
(26) Zhong, J.; Sun, G.; He, D. Classic, Liquid, and Matrix-Assisted Dip-Pen Nanolithography for Materials Research. *Nanoscale* **2014**, *6*, 12217−12228.
(27) Xie, Z.; Zhou, X.; Tao, X.; Zheng, Z. Polymer Nanostructures Made by Scanning Probe Lithography: Recent Progress in Material Applications. *Macromol. Rapid Commun.* **2012**, *33*, 359−373.
(28) Guardingo, M.; Esplandiu, M. J.; Ruiz-Molina, D. Synthesis of Polydopamine at the Femtoliter Scale and Confined Fabrication of Ag Nanoparticles on Surfaces. *Chem. Commun.* **2014**, *50*, 12548−12551.
(29) Radha, B.; Liu, G.; Eichelsdoerfer, D. J.; Kulkarni, G. U.; Mirkin, C. A. Layer-by-Layer Assembly of a Metallomesogen by Dip-Pen Nanolithography. *ACS Nano* **2013**, *7*, 2602−2609.
(30) Arrabito, G.; Reisewitz, S.; Dehmelt, L.; Bastiaens, P. I.; Pignataro, B.; Schroeder, H.; Niemeyer, C. M. Biochips for Cell Biology by Combined Dip-Pen Nanolithography and DNA-Directed Protein Immobilization. *Small* **2013**, *9*, 4243−4249.
(31) Hernandez-Santana, A.; Irvine, E.; Faulds, K.; Graham, D. Rapid Prototyping of Poly(dimethoxysiloxane) Dot Arrays by Dip-Pen Nanolithography. *Chem. Sci.* **2011**, *2*, 211−215.
(32) Brinkmann, F.; Hirtz, M.; Greiner, A. M.; Weschenfelder, M.; Waterkotte, B.; Bastmeyer, M.; Fuchs, H. Interdigitated Multicolored Bioink Micropatterns by Multiplexed Polymer Pen Lithography. *Small* **2013**, *9*, 3266−3275.
(33) Bellido, E.; González-Monje, P.; Repollés, A.; Jenkins, M.; Sesé, J.; Drung, D.; Schurig, T.; Awaga, K.; Luis, F.; Ruiz-Molina, D. Mn_{12} Single Molecule Magnets Deposited on μ-SQUID Sensors: The Role of Interphases and Structural Modifications. *Nanoscale* **2013**, *5*, 12565−12573.
(34) Martínez-Pérez, M. J.; Bellido, E.; De Miguel, R.; Sesé, J.; Lostao, a.; Gómez-Moreno, C.; Drung, D.; Schurig, T.; Ruiz-Molina, D.; Luis, F. Alternating Current Magnetic Susceptibility of a Molecular Magnet Submonolayer Directly Patterned onto a Micro Superconducting Quantum Interference Device. *Appl. Phys. Lett.* **2011**, *99*, 032504.
(35) Domingo, N.; Bellido, E.; Ruiz-Molina, D. Advances on Structuring, Integration and Magnetic Characterization of Molecular Nanomagnets on Surfaces and Devices. *Chem. Soc. Rev.* **2012**, *41*, 258−302.
(36) Bellido, E.; Cardona-Serra, S.; Coronado, E.; Ruiz-Molina, D. Assisted-Assembly of Coordination Materials into Advanced Nanoarchitectures by Dip-Pen Nanolithography. *Chem. Commun.* **2011**, *47*, 5175−5177.
(37) Carbonell, C.; Imaz, I.; Maspoch, D. Single-Crystal Metal−Organic Framework Arrays. *J. Am. Chem. Soc.* **2011**, *133*, 2144−2147.
(38) Carbonell, C.; Stylianou, K. C.; Hernando, J.; Evangelio, E.; Barnett, S. A.; Nettikadan, S.; Imaz, I.; Maspoch, D. Femtoliter Chemistry Assisted by Microfluidic Pen Lithography. *Nat. Commun.* **2013**, *4*, 2173.
(39) Inorganic nanoparticles have already been synthesized by delivering their precursors using tip-assisted methodologies, for example in: Liu, G.; Eichelsdoerfer, D. J.; Rasin, B.; Zhou, Y.; Brown, K. A.; Liao, X.; Mirkin, C. A. Delineating the Pathways for the Site-Directed Synthesis of Individual Nanoparticles on Surfaces. *Proc. Natl. Acad. Sci. U. S. A.* **2013**, *110*, 887−891.
(40) Guardingo, M.; Busqué, F.; Novio, F.; Ruiz-Molina, D. Design and Synthesis of a Non Innocent Multitopic Catechol and Pyridine Mixed Ligand: Nanoscale Polymers and Valence Tautomerism. *Inorg. Chem.* **2015**, *54*, 6776−6781.
(41) Liu, G.; Zhou, Y.; Banga, R. S.; Boya, R.; Brown, K. A.; Chipre, A. J.; Nguyen, S. T.; Mirkin, C. A. The Role of Viscosity on Polymer Ink Transport in Dip-Pen Nanolithography. *Chem. Sci.* **2013**, *4*, 2093−2099.
(42) Bellido, E.; de Miguel, R.; Ruiz-Molina, D.; Lostao, A.; Maspoch, D. Controlling the Number of Proteins with Dip-Pen Nanolithography. *Adv. Mater.* **2010**, *22*, 352−355.

DOI: 10.1021/acsnano.5b05071
ACS Nano XXXX, XXX, XXX−XXX